

Study of Electronic Properties of Bismuth- Antimony ($\text{Bi}_{1-x}\text{Sb}_x$) Nanowire

Vishwajeet Kumar Chandel¹, K. B. Singh², Om Prakash Singh³

¹Research Scholar, Department of Physics, J. P. University, Chapra, Bihar, India

²Department of Physics, L. S. College, Muzaffarpur, B. R. A. Bihar University, Muzaffarpur, Bihar, India

³Department of Physics, J. P. University, Chapra, Bihar, India

ABSTRACT

In this paper, we presented about the study of the bismuth antimony ($\text{Bi}_{1-x}\text{Sb}_x$) alloys material are considered to be one of the best materials for low temperature thermoelectrics, supercooling, millivolt electronics and infrared applications. A notable number of interesting properties have been observed in bulk bismuth materials, such as non-parabolic dispersions and abnormal magneto-resistance, the ultra-high mobility of carriers, and the high anisotropy. In 1993, Hicks et al. suggested that thermoelectric materials could have enhanced figure of merit if the materials were synthesized in the form of low dimensional systems and nano-systems. Since then, much more focus has been given to bismuth antimony as related to nanoscience and nanotechnology. Keywords : Nanowire, Bismuth- Antimony, quantum Confinement Effect.

Article Info

Volume 9, Issue 2

Page Number : 284-288

Publication Issue

March-April-2022

Article History

Accepted : 01 April 2022

Published : 12 April 2022

I. INTRODUCTION

Lin et al. have synthesized and studied some electronic properties of $\text{Bi}_{1-x}\text{Sb}_x$ nanowires of diameters ($d=40, 45$ and 60 nm) and Sb composition ($x=0, 0.05, 0.10$ and 0.15), which are oriented along the (012) crystalline axis. 1-5 $\text{Bi}_{1-x}\text{Sb}_x$ nanowires with their wire axis oriented in the trigonal direction have been studied by Rabin et al, 6 for the composition range of ($x=0\sim 0.30$) and the nanowire diameter range ($d=10\sim 100$ nm), below the temperature of 77 K, where the authors suggested that the thermoelectric performance can be optimized by aligning the carrier pockets. $\text{Bi}_{1-x}\text{Sb}_x$ wires of larger diameters on the order of microns have been studied

for their strain effect in the wire direction on their electrical resistivity by Nikolaeva et al. 7 Tang and Dresselhaus have given systematic guidance on the electronic band structure of $\text{Bi}_{1-x}\text{Sb}_x$ thin films as a function of growth orientation, film thickness, stoichiometry and temperature.8,9,10 However, there are no corresponding systematic studies of $\text{Bi}_{1-x}\text{Sb}_x$ nanowires, and researchers, especially experimentalists, are very eager for global guidance on $\text{Bi}_{1-x}\text{Sb}_x$ nanowires as a function of growth orientation, wire diameter, stoichiometry, temperature, etc. The present paper aims to provide such guidance on the electronic phases and band gaps or band overlaps of $\text{Bi}_{1-x}\text{Sb}_x$ nanowires to stimulate

the synthesis of such nanowires for different applications.

In the current paper, we first develop a model for the mini-band gap and the related non-parabolic dispersion relations at the L point of bismuth antimony in one dimension. In particular we use the iterative one dimensional two band model, and we have here developed an analytical approximation for this model. Thereafter, we study the band edges and electronic phases as a function of growth orientation, wire diameter and stoichiometry, including the semimetal phases, the indirect semiconductor phases and the direct semiconductor phases. The band overlap of the semimetal phases, and the band gap of the semiconductor phases are then studied as well. The aim of this paper is to: 1) develop a one-dimensional non-parabolic band model, and 2) provide a guide for the synthesis of Bi_{1-x}Sb_x nanowires with various crystallographic orientations that could be used for different applications.

II. MATERIALS AND METHODS

We first review the crystal and electronic band structure of bulk materials of Bi_{1-x}Sb_x. The bulk materials of bismuth, antimony and their alloys have the same R3m symmetry with a rhombohedral lattice structure.

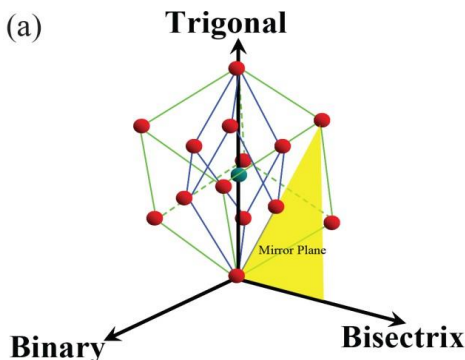


Figure 1 : The atomic unit cell of bismuth

The quantum confinement effect of nanowires may change the symmetry properties of the carrier

pockets, the positions in energy of the band edges, and possibly the shape of the dispersion relations at the *T* point, the *L* points and the *H* points. There are two types of quantum confinement effects on the band edges. One is a trivial quantum confinement effect that does not change the inverse-effective-mass tensor or the shape of the dispersion; the other is a non-trivial quantum confinement effect that does change the inverse-effective-mass tensor and the shape of the dispersion. For the *T* point and the *H* points, the dispersions of the band edges are parabolic, and the quantum confinement effect is trivial. The valence band edge at the *T* point will decrease in energy by $\frac{\hbar^2}{8} \cdot (d_1^{-2} \cdot \alpha_{||,11}^{[T,Wire]} + d_1^{-2} \cdot \alpha_{||,22}^{[T,Wire]})$ where d_1 and d_2 are the cross-sectional widths of a rectangular nanowire, and $\alpha_{||,11}^{[T,Wire]}$ and $\alpha_{||,22}^{[T,Wire]}$ are the corresponding components of the cross-sectional inverse-effective-mass tensor.¹¹ For a square nanowire, the width is $d=d_1=d_2$, and the expression of energy decrease at the *T* point is reduced to $\frac{\hbar^2}{8^2} \cdot (\alpha_{||,11}^{[T,Wire]} + \alpha_{||,22}^{[T,Wire]})$. Similarly, the valence band edge at an *H* point will decrease in energy by $\frac{\hbar^2}{8} \cdot (d_1^{-2} \cdot \alpha_{||,11}^{[H,Wire]} + d_1^{-2} \cdot \alpha_{||,22}^{[H,Wire]})$ for a rectangle nanowire, and by $\frac{\hbar^2}{8^2} \cdot (\alpha_{||,11}^{[H,Wire]} + \alpha_{||,22}^{[H,Wire]})$ for a square nanowire. Furthermore, we can still assume that $\alpha_{||,11}^{[T,Wire]} = \alpha_{||,11}^{[T,Bulk]}$ and $\alpha_{||,11}^{[H,Wire]} = \alpha_{||,11}^{[H,Bulk]}$ as have been validated in previous reports.^{5,6,8,9}

For the *L* points, the dispersions of the band edges are non-parabolic, and the quantum confinement effect is non-trivial, so that the traditional square-well model is not accurate any more. There coexists an electron pocket and a hole pocket at each *L* point. Thus, the conduction band edge and the valence band edge for the *L* point are very close to each other in energy, and are strongly coupled, which results in the non-parabolicity of the dispersion for the *L*-point electrons and holes or possibly even linearity if the two bands

are touching. Meanwhile, the shape of the dispersion is also correlated with the magnitude of the narrow band gap. On the one hand, quantum confinement in the cross-sectional plane will change the narrow band gap, which is associated with the inverse-effective-mass tensor. On the other hand, the inverse-effective-mass tensor of Bi_{1-x}Sb_x nanowire is changed by the change of the narrow band gap, which is also different from the inverse-effective-mass tensor of a bulk Bi_{1-x}Sb_x with the same Sb composition. Therefore, the puzzle is that neither the narrow band gap nor the inverse effective-mass tensor is known at this stage for the nanowires case.

Historically, the relation between the narrow band gap and the dispersion for bulk bismuth is described by a two-band model¹⁶

$$p \cdot \alpha^{[L,Bulk,Bi]} \cdot p = E(k) \left(1 + \frac{E(k)}{E_g^{[L,Bulk,Bi]}} \right), \quad (1)$$

Where $\alpha^{[L,Bulk,Bi]}$ is the inverse-effective mass tensor for the L point carrier-pocket of bulk bismuth, and it is assumed that $\alpha^{[L,Bulk]}$ for both the conduction band edge and the valence band edge are the same due to the strong interaction between these two bands and this approximation has been shown to be valid for bulk bismuth samples. The relation between the band gap and the inverse effective mass tensor is seen more clearly in the form of the second derivative of Eq. (1),

$$\alpha^{[L,Bulk,Bi]} = \frac{2}{\hbar^2} \frac{\partial^2}{\partial k^2} = \frac{1}{m} I \pm \frac{1}{m_0^2} \frac{2}{E_g^{[L,Bulk,Bi]}} p^2 \quad (2)$$

where m_0 is the mass of free electron and I is the identity matrix. It is assumed that the form of Eq. (2) holds also for Bi_{1-x}Sb_x in the range of $x = 0 \sim 0.30$, though the band gap and the effective mass tensor may change as a function of Sb composition x . Thus, we further have [5,18]

$$\alpha^{[L,Bulk,Bi_{1-x}Sb_x]} = \frac{E_g^{[L,Bulk,Bi_{1-x}Sb_x]}}{E_g^{[L,Bulk,Bi]}} \left(\alpha^{[L,Bulk,Bi]} - \frac{1}{m_0} I \right) + \frac{1}{m_0} I \quad (3)$$

which is consistent with the experimental results carried out by Mendez et al, where a simpler version of Eq. (3) was adopted¹⁹ and is given by,

$$\alpha^{[L,Bulk,Bi_{1-x}Sb_x]} = \frac{E_g^{[L,Bulk,Bi_{1-x}Sb_x]}}{E_g^{[L,Bulk,Bi]}} \alpha^{[L,Bulk,Bi]} \quad (4)$$

The theoretical validation between from Eq. (3) and Eq. (4) is discussed in Ref.⁸, and these experiences can be extended to connect the bulk materials and nanowire materials, i.e.

$$\alpha^{[L,Bulk,Bi_{1-x}Sb_x]} = \frac{E_g^{[L,Bulk,Bi_{1-x}Sb_x]}}{E_g^{[L,Bulk,Bi]}} \left(\alpha^{[L,Bulk,Bi]} - \frac{1}{m_0} I \right) + \frac{1}{m_0} I \quad (5)$$

and

$$\alpha^{[L,Bulk,Bi_{1-x}Sb_x]} = \frac{E_g^{[L,Bulk,Bi_{1-x}Sb_x]}}{E_g^{[L,Bulk,Bi]}} \alpha^{[L,Bulk,Bi]} \quad (6)$$

Now we have two approaches to solving the dispersion relation and for finding the narrow band gap of the L-point band edges. One is the iterative way. We set $E_g^{(0)} = E_g^{[L,Bulk,Bi]}$ and $\alpha^0 = \alpha^{[L,Bulk,Bi]}$ and we repeatedly carry out the iteration steps of

$$E_g^{(n+1)} = E_g^{[n]} + 2 \cdot \frac{\hbar^2}{8d^2} \cdot \text{trace} (\alpha_{||}^{(n)}) \quad (7)$$

and

$$\alpha^{(n+1)} = \frac{E_g^{(n)}}{E_g^{(n+1)}} + \left(\alpha^{(n)} - \frac{1}{m_0} I \right) + \frac{1}{m_0} I \quad (8)$$

Until convergence, where $\alpha_{||}^{(n)}$ is the cross-sectional sub-tensor of $\alpha^{(n)}$.

The other approach is to use the simple Eq. (6) and derive a solution in an analytical form, by solving Eq. (6) and

$$\begin{aligned} & E_g^{(L,Wire,Bi_{1-x},Sb_x)} \\ & = E_g^{(L,Bulk,Bi)} \\ & + 2 \cdot \frac{\hbar^2}{8d^2} \cdot \text{trace} (\alpha_{||}^{[L,Wire,Bi_{1-x},Sb_x]}) \dots (9) \end{aligned}$$

Thus, the L-Point narrow band gap of the nanowire

III. RESULTS AND DISCUSSION

Now we illustrate the electronic phase diagrams and band gap/overlap diagrams of $\text{Bi}_{1-x}\text{Sb}_x$ nanowires with a much stronger quantum confinement effect, occurring in nanowires with a small width, explicitly for nanowire with a width of 10 nm. The small width nanowires show how the quantum confinement effect influences the symmetry properties and the electronic phases of the nanowires comparatively. The electronic phase diagrams and band gap/overlap of $\text{Bi}_{1-x}\text{Sb}_x$ nanowires with $d=10$ nm, as a function of growth orientation and stoichiometry, are illustrated in Fig. 2. The changes in the electronic phase diagrams are more obvious in Fig. 2. First, the direct semiconductor phase regions have disappeared in all of the three cases (a), (b) and (c). The semimetal phase region (dark blue) where the top of the valence band edge is located at the T point has significantly shrunk to a tiny size in both Fig. 2(a) and Fig. 2(c), and has disappeared in Fig. 2(b). The semimetal phase region where the top of the valence band edge is located at an H point (light blue) has shrunk as well, in all the three cases, but still is present. The dominant phase regions become the indirect semiconductor phases, which have both expanded remarkably in Fig. 2 (a), (b) and (c). Such information is very important for the design of electronic devices using $\text{Bi}_{1-x}\text{Sb}_x$ nanowires. The much stronger quantum confinement effect in 10 nm wide nanowires makes the contrast for the anisotropy of all the diagrams much more obvious. The existence of inversion symmetry and the absence of mirror symmetry is shown clearly in Fig. 2 (a) and (d). Furthermore, the mirror symmetry about the binary axis, mirror

symmetry about the trigonal axis, and the associated inversion symmetry of the orientation-stoichiometry phase diagram of the trigonal-binary crystallographic plane normal to the bisectrix is further clarified in Fig. 2(c) and (f). The above discussions show that $\text{Bi}_{1-x}\text{Sb}_x$ nanowires of larger wire width show a much richer variation of electronic phases, but the contrast of anisotropy for different growth orientation is less obvious, while for the $\text{Bi}_{1-x}\text{Sb}_x$ nanowires of larger wire width, the richness of the variation of electronic phases is reduced, but the contrast of the anisotropy for different growth orientations is much enhanced.

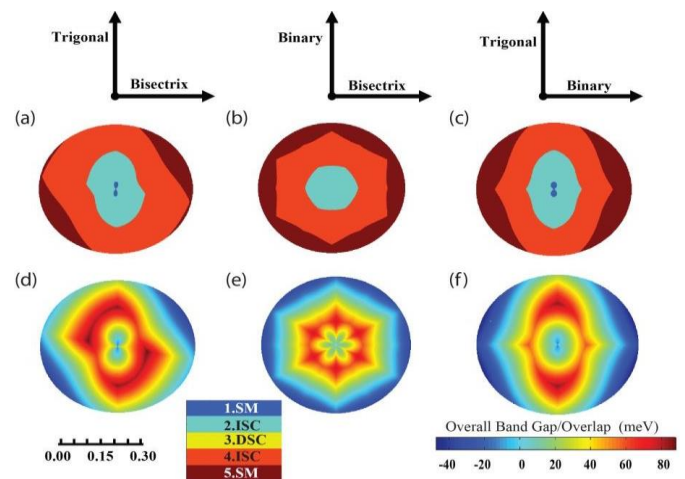


Figure 2: The electronic phase diagrams (a)-(c), and the band gap/overlap diagrams (d)-(f) of $\text{Bi}_{1-x}\text{Sb}_x$ nanowires of 10 nm wire width, as a function of wire growth orientation and Sb composition x .

IV. CONCLUSION

In conclusion, we have developed a model to accurately describe the quantum confinement in one-dimensional narrow band gap systems, which accurately captures the band edge shifts and the shape of the non-parabolic dispersion relations. We have then used this model to study the phase diagrams and band gap/overlap of the bismuth-antimony nanowire materials system.

V. REFERENCES

- [1]. HT Chu and Yi-Han Kao, Physical Review B 1 (6), 2369 (1970); HT Chu and Yi-Han Kao, Physical Review B 1 (6), 2377 (1970).
- [2]. Takehito Yazaki and Yuzo Abe, Journal of the Physical Society of Japan 24 (2) (1968); GE Smith, Physical Review Letters 9 (12), 487 (1962).
- [3]. LD Hicks and MS Dresselhaus, Phys. Rev. B 47 (19), 12727 (1993); LD Hicks and MS Dresselhaus, Phys. Rev. B 47 (24), 16631 (1993).
- [4]. Yu-Ming Lin, SB Cronin, O Rabin, Jackie Y Ying, and MS Dresselhaus, Applied physics letters 79, 677 (2001); Yu-Ming Lin, O Rabin, SB Cronin, Jackie Y Ying, and MS Dresselhaus, Applied physics letters 81 (13), 2403 (2002).
- [5]. Oded Rabin, Yu-Ming Lin, and Mildred S Dresselhaus, Applied physics letters 79, 81 (2001).
- [6]. A Nikolaeva, P Bodiul, L Konopko, and Gh Para, presented at the Thermoelectrics, 2002. Proceedings ICT'02. Twenty-First International Conference on, 2002 (unpublished); AA Nikolaeva, LA Konopko, TE Huber, PP Bodiul, IA Popov, and EF Moloshnik, Journal of Electronic Materials, 1 (2012); Albina A Nikolaeva, Leonid A Konopko, Tito E Huber, Pavel P Bodiul, and Ivan A Popov, Journal of Solid State Chemistry (2012).
- [7]. Shuang Tang and Mildred S Dresselhaus, Physical Review B 86 (7), 075436 (2012).
- [8]. Shuang Tang and Mildred S Dresselhaus, Nano letters 12 (4), 2021 (2012); Shuang Tang and Mildred S. Dresselhaus, Nanoscale 4 (24), 7786 (2012).
- [9]. Adishwar Lal Jain, Physical Review 114 (6), 1518 (1959).
- [10]. EJ Tichovolsky and JG Mavroides, Solid State Communications 7 (13), 927 (1969).
- [11]. B Lenoir, M Cassart, J-P Michenaud, H Scherrer, and S Scherrer, Journal of Physics and Chemistry of Solids 57 (1), 89 (1996).

Cite this article as :

Vishwajeet Kumar Chandel, K. B. Singh, Om Prakash Singh, "Study of Electronic Properties of Bismuth-Antimony (Bi₁-Xsbx) Nanowire", International Journal of Scientific Research in Science and Technology (IJSRST), Online ISSN : 2395-602X, Print ISSN : 2395-6011, Volume 9 Issue 2, pp. 284-288, March-April 2022. Available at doi : <https://doi.org/10.32628/IJSRST229253> Journal URL : <https://ijsrst.com/IJSRST229253>